Iranian Journal of Medical Physics

ijmp.mums.ac.ir

Fetal Dose Variations in Lung Scintigraphy of Pregnant Woman: The Role of Fetal Body Habitus

Motahareh Zohur-Karbaf[1], Hashem Miri-Hakimabad[1*], Elie Hoseinian-Azghadi[2]

1. Physics Department, Faculty of Science, Ferdowsi University of Mashhad, Mashhad, Iran.
2. Research and Education Department, Reza Radiotherapy and Oncology Center, Mashhad, Iran

ARTICLE INFO

Article type:
Original Paper

Article history:
Received: Jan 17, 2022
Accepted: June 27, 2022

Keywords:
Computational Phantom
Pregnant Phantom
Fetal Dose Coefficient
Fetal Dose Variation
Lung Scintigraphy

ABSTRACT

Introduction: This study aims to address the radiation exposure incurred by lung scintigraphy in pregnant patients suspected of pulmonary embolism and to investigate the dose variations due to different body habitus of the fetus.

Material and Methods: In this respect, seven computational models of pregnant women and fetus in three trimesters of pregnancy were used and Monte Carlo calculations were performed using Monte Carlo n-particle –extended (MCNPX) code version 2.6.0 to assess absorbed dose coefficients. Time-integrated activities for three radiopharmaceuticals considered in this study were also extracted from the available reference biokinetic data.

Results: Fetal dose coefficients (mGy/MBq) for three radiopharmaceuticals labeled with 99*m*Tc were estimated for reference pregnant phantoms at three trimesters of gestation and 10*th*, and 90*th* fetal growth percentiles were also considered during the last two trimesters. The results show that the fetal dose coefficients were 2.09×10^{-2}, 5.71×10^{-3}, and 4.44×10^{-3} mGy/MBq for ^{99m}Tc MAA, 8.31×10^{-4}, 8.68×10^{-4}, and 1.27×10^{-3} mGy/MBq for ^{99m}Tc Technegas, and 7.85×10^{-3}, 2.42×10^{-3}, and 2.66×10^{-3} mGy/MBq for ^{99m}Tc DTPA aerosol, respectively. According to the results the factor of fetal body habitus adds variation to the fetal dose within ±15%.

Conclusion: Considering one of the uncertainty components of fetal dose, that is the fetal body habitus, the dose variations were well below the safety threshold for the fetus (the threshold from ICRP Publication 84 for fetal cancer risk). Therefore, to check the safety of the diagnostic examination in terms of radiation dose to the fetus, it is sufficient to take into account the reference dose values in clinical practice.

►*Please cite this article as:*
Zohur-Karbaf M, Miri-Hakimabad H, Hoseinian-Azghadi E. Fetal Dose Variations in Lung Scintigraphy of Pregnant Woman: The Role of Fetal Body Habitus. Iran J Med Phys 2023; 20: 184-193. 10.22038/IJMP.2022.63048.2069.

Introduction

Pulmonary embolism (PE) in pregnant patients is potentially fatal and is still one of the leading causes of maternal mortality worldwide even in developed countries [1]. Over 1 death per 100,000 deliveries are related to pregnancy-associated PE, which accounts for a reported range of 10%-20% of maternal deaths. According to literature, the risk of PE in pregnant women is 6 times greater than that for nonpregnant women [1, 2]. Mismanagement of PE can lead to higher mortality rates, while early and accurate diagnosis and appropriate management subsequently can result in reduced mortality [3-6]. Moreover, the first 30 minutes after the sentinel event is crucial for saving the pregnant patient and this short period makes it more difficult for clinicians to intervene in a timely and accurate fashion [7].

Lung scintigraphy is a key component of diagnostic clinical pathway recommended by seven international guidelines for investigation of suspected PE in pregnant patients [8-13]. However, it is not always the primary advanced imaging test, but often suggests when the result of chest radiograph is negative. Lung scintigraphy is typically performed as ventilation and perfusion scans. In case of pregnancy, perfusion scan is typically the only performed test because of radiation exposure concerns for the fetus, except those with abnormal perfusion scan. Dealing with diagnostic examinations using ionizing radiation, such as perfusion/ventilation scans, one of the major concerns for the physician is radiation exposure to both the pregnant woman and fetus. In particular, many authors addressed the amount of radiation dose incurred by lung scintigraphy in the past two decades [7, 14-19]. However, the amount of radiation dose is dependent on many factors such as anatomical and physiological parameters of both pregnant woman and the fetus, the uncertainty components were not fully investigated yet.

Therefore, in this study we aimed to investigate the effect of different fetal body habitus subgroups on fetal dose. Furthermore, we aimed to investigate whether the dose variation is clinically relevant. The answer of this question determines if we have to assess the fetal doses separately for each fetal growth

*Corresponding Author: Tel: 051-38804099; Email: mirihakim@um.ac.ir

percentile. In fact, this study intends to computationally specify the dose variations due to one of the uncertainty components (i.e., geometrical different size of the fetus).

Materials and Methods

Phantom

The phantoms used in this study were 3-, 6-, and 9-month pregnant models (Figure 1). The 3-month pregnant phantom only contains the fetus at 50th percentile, while, the 6- and 9- month pregnant models include fetal models at 10th, 50th and 90th statistical percentiles. The fetal models at 10th and 90th percentiles were constructed based on the rescaled 50th model using biometry data tables (more details about construction of fetal models were given by reference [20].

The mass of the fetal and maternal organs and tissues correspond to the reference masses reported by the International Committee for Radiation Protection [21]. The total weight of the pregnant models was 60.8, 65.5, and 68.1 kg for 3-, 6-, and 9-month gestational ages, respectively. The voxel dimensions of 6- and 9-month phantoms are (1.775 × 1.775 × 4.84 mm^3), whereas the voxel dimensions of the 3-month pregnant phantom are (0.8875 × 0.8875 × 1.21 mm^3). The total masses of fetal models at 50th percentile were 0.097, 0.995, and 3.47 kg for 3-, 6-, and 9-month, respectively. The used fetal models contain 20 different organs and tissues [20, 22, 23].

Internal dose calculation

The absorbed dose coefficient to target organ d (r_T) in mGy/MBq is calculated as:

$$d(r_T) = \sum_S \frac{\tilde{A}_S}{A_0} S(r_T \leftarrow r_S) \quad (1)$$

Where S factor, $S(r_T \leftarrow r_S)$, is the mean absorbed dose to the target region r_T per unit of nuclear transition of the relevant radionuclide in the source region r_S in unit (mGy MBq^{-1} h^{-1}). $\tilde{A}_S$ (MBq h) is the time-integrated activity or the activity accumulated in the source organ or tissue, S, and A_0 (MBq) is the administered activity to the patient. Figure 2 indicates a flowchart including all the steps to be followed for internal dose calculations.

S factors. In order to calculate the S factor, $S(r_T \leftarrow r_S)$, a computational phantom, i.e., a virtual simulation of human body with its organs and tissues is needed. The incorporation of computational phantom into the Monte Carlo code enables us to calculate the quantity named S factor. The MCNPX code version 2.6.0 was used [24] to estimate $S(r_T \leftarrow r_S)$ for several pairs of source-target organs in this study. The CEL keyword was used in the source definition (SDEF) card to define the specified source organs. The method of defining the source was previously described by Taranenko et al. [25] in detail. Source organs were defined as maternal bladder contents, kidneys, liver, esophagus, oral mucosa, salivary glands, small intestine contents, colon contents, stomach wall and contents, thyroid, uterus, other tissues, placenta, amniotic fluid, and fetal ossified bones, other tissues, and thyroid. The number of particle histories was selected to be 10^9 and absorbed dose was scored by tally F6: p when source particles are photons and +F6 when source particles are electrons. By using *F8 tally and dividing the results by the mass of the organ, similar values would be obtained, as previously mentioned by other authors [26]. The statistical errors for tally values were less than 3%.

Biokinetic data. The time-integrated activity for each source organ, S, is defined as:

$$\tilde{A}_S = \int_0^\infty A_s(t)dt \quad (2)$$

Where t is the time after radionuclide administration, and $A_s(t)$ is the activity of source organ at time t. The amount of $A_s(t)$ is determined by mathematical models called biokinetic models. The biokinetic models are reference models, which are determined by (1) physiology of patient's body, and (2) the chemical properties of radiopharmaceutical. In this study, three types of scans were assumed: (1) perfusion scan with ^{99m}Tc-MAA, (2) perfusion/ventilation scan with ^{99m}Tc-MAA/^{99m}Tc-technegas, and (3) perfusion/ventilation scan with ^{99m}Tc-MAA/^{99m}Tc- DTPA. The biokinetic data for ^{99m}Tc-MAA and ^{99m}Tc- DTPA were extracted from [27]. In case of Tc-99m-technegas, the same assumption as was considered [18].

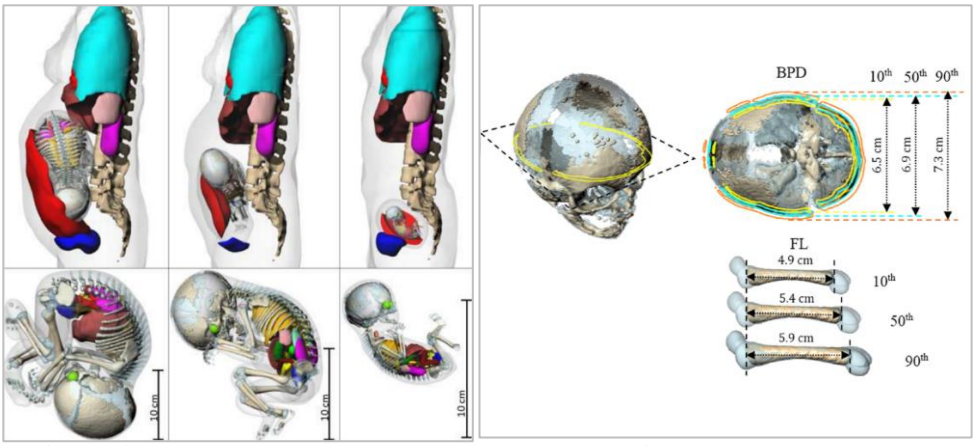

Figure 1. (a) A view of series of pregnant woman computational phantoms developed by Rafat-Motavalli et al. [21-23], (b) The biparietal diameters (BPD) and femur lengths (FL) of the 6-month models for different percentiles.

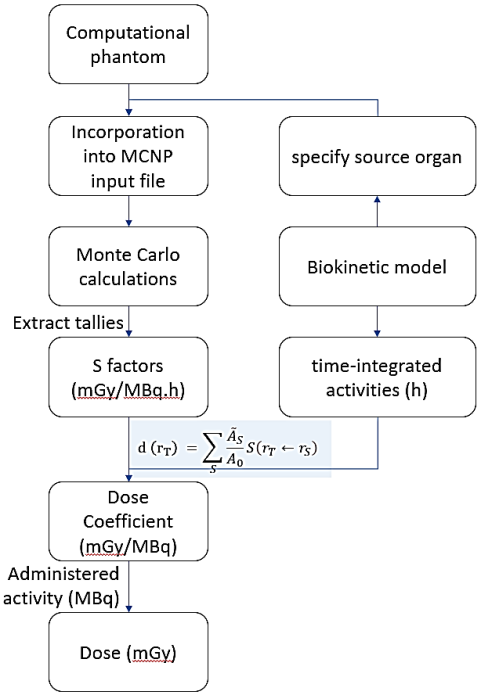

Figure 2. The followed steps for internal dose calculations in this study.

Since the available biokinetic data in the literature is for reference phantoms, therefore, in case of 10th and 90th fetal growth percentiles, two additional assumptions were made. Firstly, for a given gestational age, the time-integrated activity was assumed the same for all percentile groups. This approach called "*constant time-integrated activity*", because a constant value of time-integrated activity was assumed for 10th, 50th and 90th fetal models. Secondly, the time-integrated activity was assumed to be scaled according to the volume of fetal organs and tissues with respect to the 50th percentile. This approach was called the "*volume-based time-integrated activity*" all along the manuscript.

Dose-point kernel (DPK)

In this study, a computational estimate (DPK) dose has been used to validate the process of S factor through using Monte Carlo calculations and to justify the differences of the S factors obtained for various statistical percentiles. This quantity gives a simple estimation of the dose to water from both scattered photons and secondary electrons set in motion by primary photon interactions at one particular point.

$$DPK \propto \frac{e^{-\mu x}}{x^2} \times B(\mu x) \quad (3)$$

The dependence of the function (DPK) on the distance x is obtained by the product of an exponential attenuation term $e^{-\mu x}$, the inverse of the square of the distance term (x^{-2}), and a buildup term ($B(\mu x)$). Where μ is the attenuation coefficient, x is the distance between points either within source or target organs, and B is the buildup factor, and is a function of μx.

In order to calculate x in function (3), 10^4 points were randomly sampled in either the source and target organs, and the chord length between them was calculated. The buildup factor B is a function depending on μx which was interpolated between data reported by Martin [28]. Attenuation coefficient μ for soft tissue material and emitted photons from 99mTc were available from XCOM database [29].

Results

Dose coefficients

Fetal dose coefficients (mGy/MBq) for three radiopharmaceuticals labeled with ^{99m}Tc were estimated using seven pregnant phantoms at three gestational ages (i.e., one 3-month pregnant phantom at 50th fetal percentile, three 6-month pregnant phantoms at 10th, 50th and 90th fetal percentiles, and three 9-month pregnant phantoms at 10th, 50th and 90th fetal percentiles). The entire data for fetal dose coefficients are presented in supplementary data tables, however, the summarized information is also provided in figure 3, and table 1.

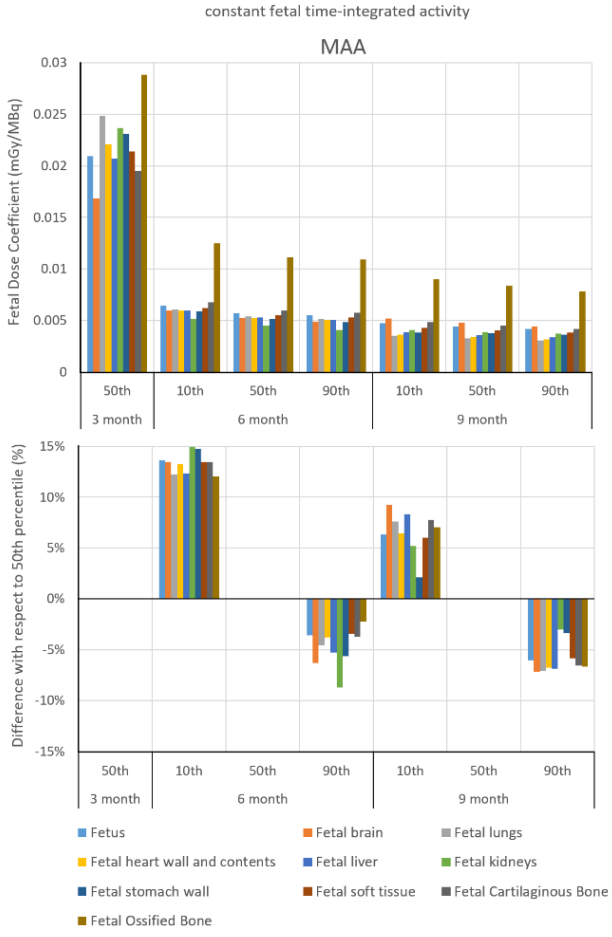

Figure 3. (a) Fetal dose coefficients to total body of the fetus and several fetal organs are included together with the differences (%) between two extreme percentiles (10th and 90th) and the reference fetal percentile (50th) for MAA administration. The statistical error bars for Monte Carlo based data in figure 3 are too small to be visible.

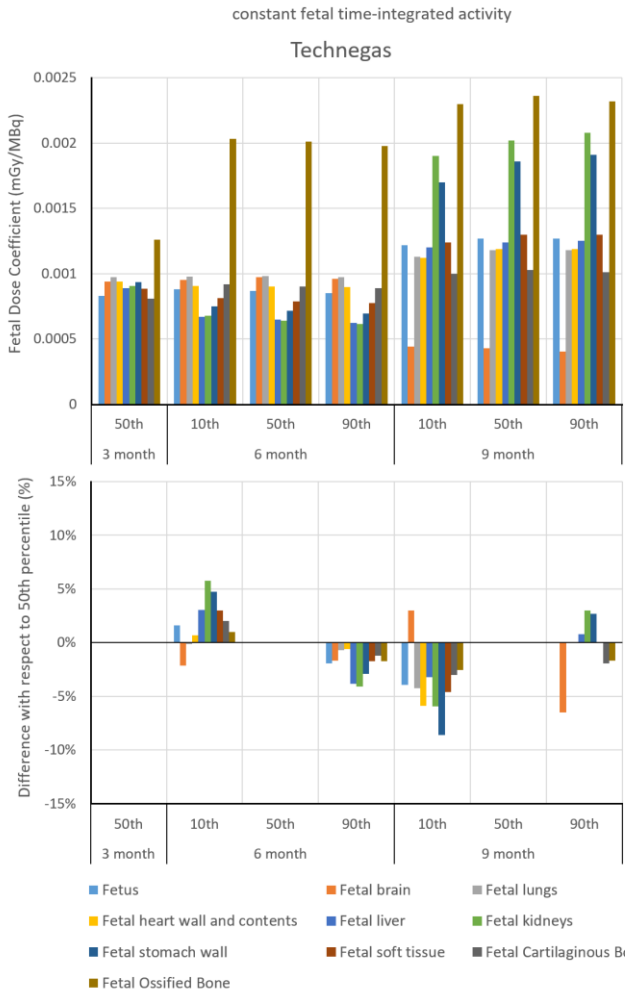

Figure 3. (b) Fetal dose coefficients to total body of the fetus and several fetal organs are included together with the differences (%) between two extreme percentiles (10th and 90th) and the reference fetal percentile (50th) for Technegas administration. The statistical error bars for Monte Carlo based data in figure 3 are too small to be visible.

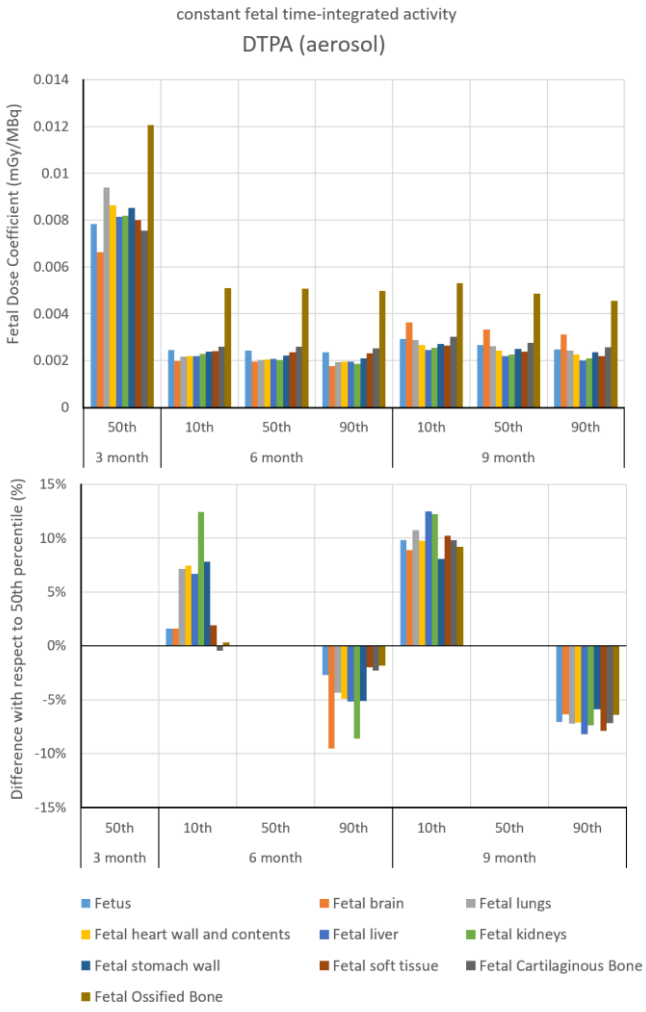

Figure 3. (c) Fetal dose coefficients to total body of the fetus and several fetal organs are included together with the differences (%) between two extreme percentiles (10th and 90th) and the reference fetal percentile (50th) for DTPA – aerosol administration. The statistical error bars for Monte Carlo based data in figure 3 are too small to be visible.

Table 1. The summary of dose coefficients and their differences (%) with respect to 50th percentile.

	Dose coefficient (mGy/MBq)						
	3-month		6-month			9-month	
	P-50	P-10	P-50	P-90	P-10	P-50	P-90
MAA:							
Fetus	2.09E-02	6.49E-03	5.71E-03	5.50E-03	4.72E-03	4.44E-03	4.17E-03
Fetal ossified bones	2.88E-02	1.25E-02	1.11E-02	1.09E-02	8.99E-03	8.40E-03	7.84E-03
Technegas:							
Fetus	8.31E-04	8.82E-04	8.68E-04	8.51E-04	1.22E-03	1.27E-03	1.27E-03
Fetal ossified bones	1.26E-03	2.03E-03	2.01E-03	1.98E-03	2.30E-03	2.36E-03	2.32E-03
DTPA aerosol:							
Fetus	7.85E-03	2.46E-03	2.42E-03	2.35E-03	2.92E-03	2.66E-03	2.47E-03
Fetal ossified bones	1.21E-02	5.09E-03	5.07E-03	4.98E-03	5.31E-03	4.86E-03	4.55E-03

Table 1. Continued.

	Difference (%) with respect to 50th percentile			
	6-month		9-month	
	P-10	P-90	P-10	P-90
MAA:				
Fetus	13.6%	3.6%-	6.3%	-6.0%
Fetal ossified bones	12.0%	-2.3%	7.0%	-6.6%
Technegas:				
Fetus	1.6%	-1.9%	-3.9%	0%
Fetal ossified bones	1.0%	-1.7%	-2.5%	-1.7%
DTPA aerosol:				
Fetus	1.6%	-2.7%	9.8%	-7.1%
Fetal ossified bones	0.3%	-1.8%	9.2%	6.4%-

The results show that the fetal dose coefficients were 2.09×10^{-2}, 5.71×10^{-3}, and 4.44×10^{-3} mGy/MBq for ^{99m}Tc MAA and for reference phantoms (50th percentile) at 3-, 6-, and 9-month gestational ages, respectively. Those for ^{99m}Tc Technegas were 8.31×10^{-4}, 8.68×10^{-4}, and 1.27×10^{-3} mGy/MBq, and for ^{99m}Tc DTPA aerosol were 7.85×10^{-3}, 2.42×10^{-3}, and 2.66×10^{-3} mGy/MBq, respectively. A comparison between the data obtained for 50th percentile and those reported by other investigators were presented in supplementary figures S1 and S2. It should be noted that the others investigators used the mathematical pregnant phantoms for dose calculations. This issue is the reason that similar dose values are reported by all of them. The important difference between this study and previous studies was observed for 3-month pregnant phantom which will be discussed in the next section, other dose coefficient values have the same order of magnitude.

In figure 3, dose coefficients to total body of the fetus and several fetal organs are included together with the differences (%) between two extreme percentiles (10th and 90th) and the reference fetal percentile (50th). It was shown that the dose coefficients decrease with increasing fetal percentile for ^{99m}Tc-MAA and aerosol ^{99m}Tc-DTPA, however, an obvious increasing or decreasing trend was not observed for ^{99m}Tc-Technegas. This issue will be discussed in the next section. The differences between the two extreme percentiles and the reference fetal percentile were up to (-8%, +15%) for 6 months and up to (-10%, +11%) for 9 months. In summary, it could be concluded that according to the results the factor of fetal body habitus adds variation to the fetal dose within ±15%.

The fetal dose coefficients for different fetal percentiles are estimated with a critical assumption about fetal time-integrated activities, and that is using a constant time-integrated activity for all percentiles at the same age. Additionally, a reasonable assumption would be a volume-based time-integrated activity varying with respect to the 50th percentile. The fetal dose coefficients using these two assumptions were also estimated and presented in figure 4. This figure shows that the volume-based time-integrated activities lead to up to about 40% less dose coefficients for approximately all considered phantoms and radiopharmaceuticals.

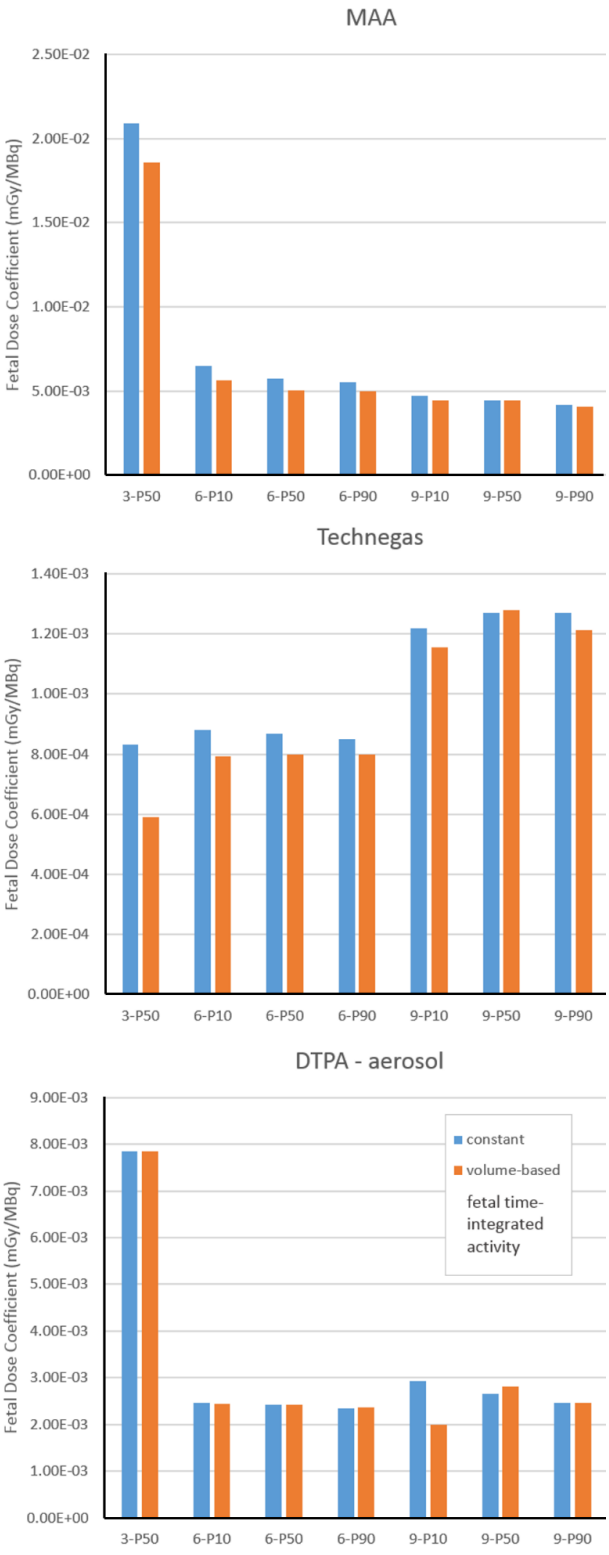

Figure 4. The fetal dose coefficients for different fetal percentiles are estimated with constant time-integrated activity and volume-based time-integrated activities. The statistical error bars for Monte Carlo based data in figure 3 are too small to be visible.

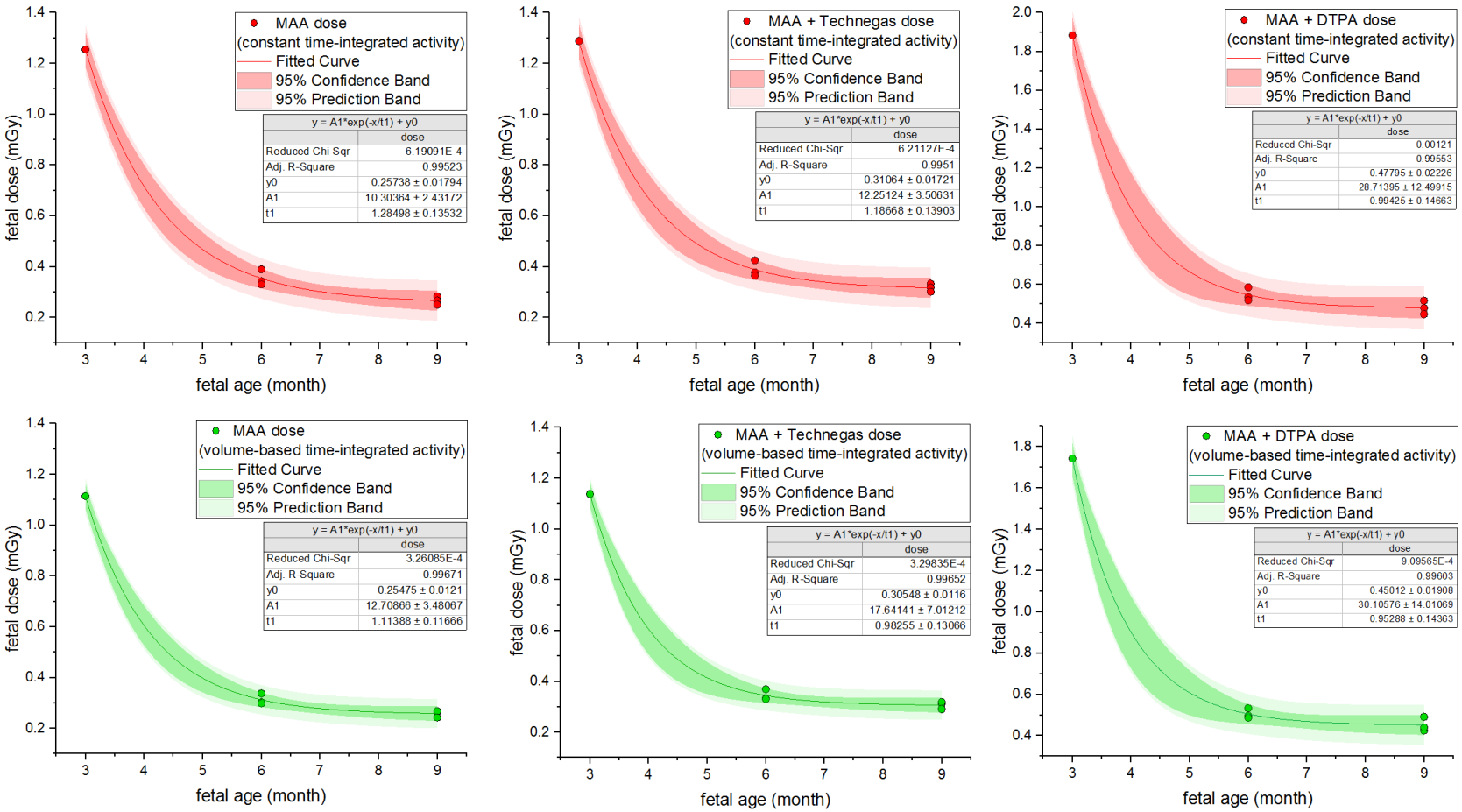

Figure 5. The dose data estimated, and 10th and 90th percentile was included to produce confidence and prediction bands with using constant time-integrated activity and volume-based time-integrated activities for administration of (a) MAA, (b) MAA and Technegas, and (c) MAA and DTPA-aerosol.

Absorbed doses

Considering the typical administered activities for each radiopharmaceutical, the absorbed doses were obtained. Figure 5 shows all the estimated dose data, and 10th and 90th percentile was included to produce confidence and prediction bands. This figure also shows the estimated data assuming volume-based time-integrated activities. It was shown that only the (^{99m}Tc-MAA) dose to 3-month fetus is greater than 1mGy and other gestational ages and fetal percentiles are well below the safe threshold of <1mGy. In addition, if we consider a ventilation-perfusion scan using both aerosol ^{99m}Tc-DTPA and ^{99m}Tc-MAA radiopharmaceuticals, the dose to ossified bones of 6-month fetus would also be higher than 1mGy.

Discussion

Firstly, we consider the 50th percentile phantoms and make a comparison between the corresponding data with literature. Considering the comparison between dose coefficients presented by this study and those reported by other investigators, a large difference was observed for 3-month pregnant phantom. Other dose coefficient values have the same order of magnitude and therefore they are in agreement with each other (supplementary figures S1 and S2). This difference highlights the importance of fetal body geometry with respect to maternal source organs and tissues. This issue is the reason that the dose coefficients for the 3-month fetus is about 5-times larger than that reported by Russell et al. and other investigators [14-16, 27, 31-32]. One of the source regions that was not included in mathematical version of 3-month pregnant phantom is the placenta, which is included in the current phantom series used in this study (see figure 1). In addition, according to supplementary figure S3, the contribution of placenta as source region to fetal dose coefficients (^{99m}Tc MAA) is particularly large (for example, 63% for 3-month fetus). Without considering the placenta, the assigned activity would be distributed in other organs, which leads to reduction of the fetal dose coefficient up to 54%. This is the major reason that led to underestimation of previously reported fetal dose coefficients. Further discussion on this issue could be find in Rafat et al. [18].

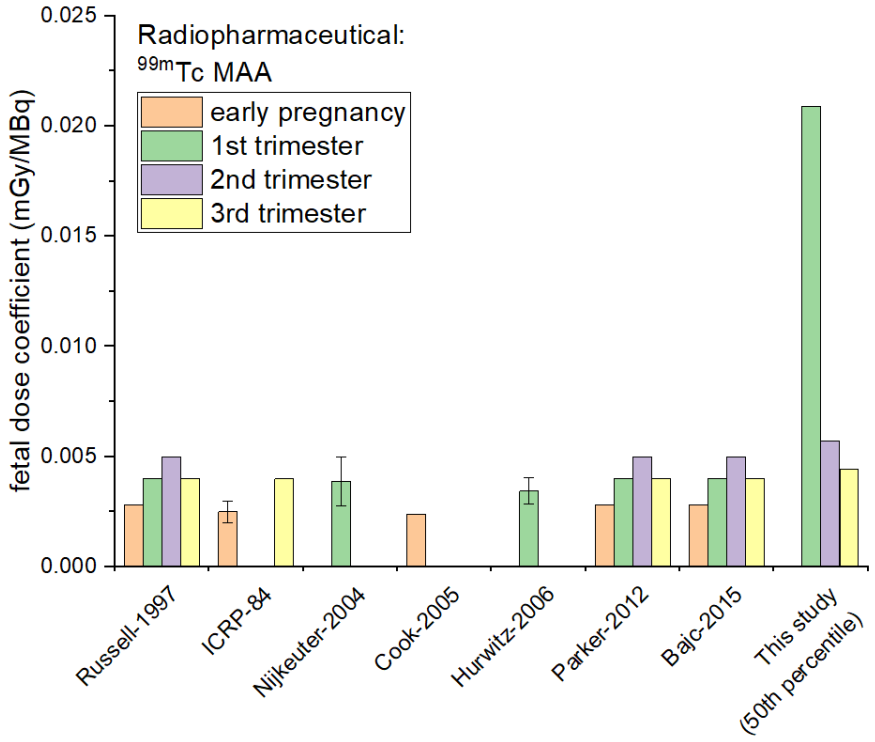

Figure S1. The fetal dose coefficients from literature in comparison with this study (50th percentile) for administration of ^{99m}Tc MAA. ICRP Publication 84, Nijkeuter et al. and Hurwitz et al. reported a range of data which was shown by error bars.

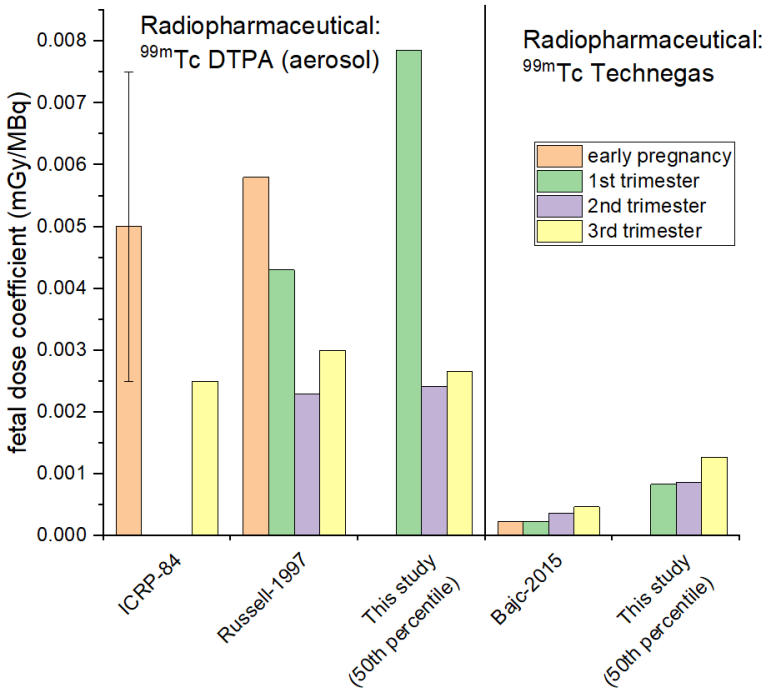

Figure S2. The fetal dose coefficients from literature in comparison with this study (50th percentile) for administration of ^{99m}Tc DTPA (aerosol), and Technegas. ICRP Publication 84 reported a range of data which was shown by error bar.

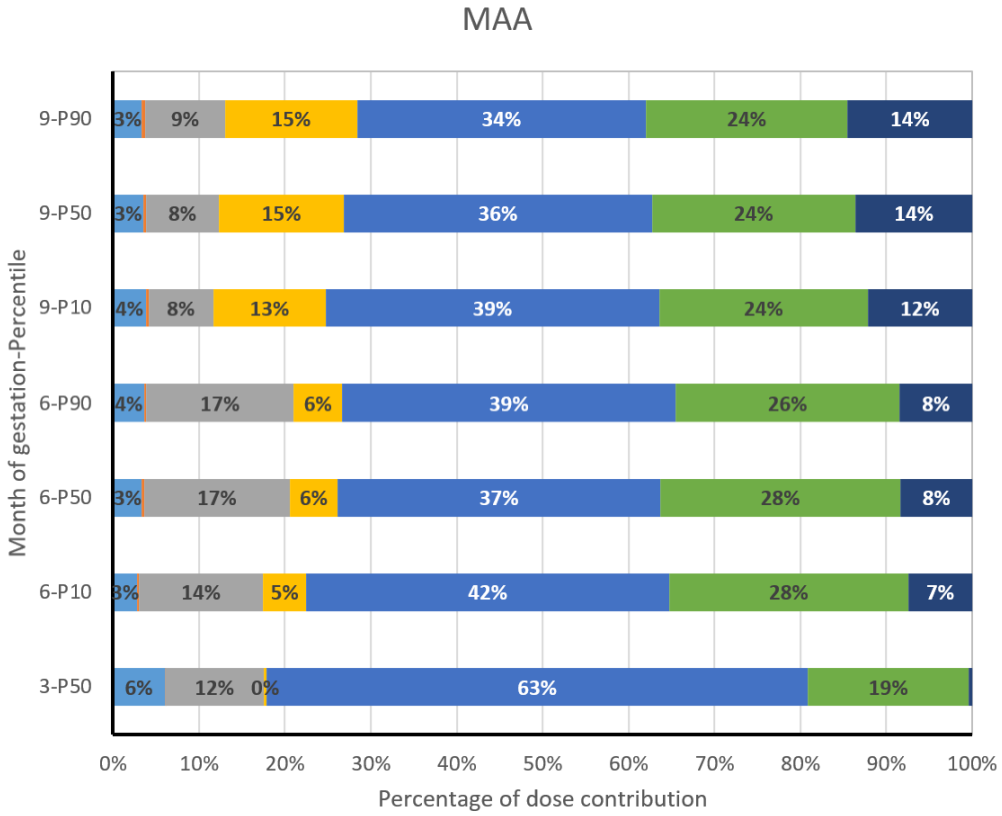

Figure S3. The percentage of dose contributions to the fetus from various source organs for administration of ^{99m}Tc MAA.

Secondly, we aimed to discuss the difference that fetal body habitus could impose to the problem. In case of ^{99m}Tc-MAA and aerosol ^{99m}Tc-DTPA administration, the fetal dose coefficients decreased with increasing fetal percentile. To address this issue, the contribution of source organs to fetal dose coefficients should be determined. As an example, figure 6 shows the contribution of source organs to fetal dose coefficients

for administration of ^{99m}Tc-DTPA (aerosol) to pregnant women at the third trimester of gestation (with fetuses at 10th, 50th and 90th percentile). According to this figure, the maternal lung is the major contributor (~80%) to fetal dose and therefore, the distance between the fetus and maternal lung plays an important role in determining the amounts of fetal dose coefficients. To obtain the distances between the fetus and maternal lung, the chord length distributions between these two organs were obtained to be used in the estimation of dose point kernel values. By using dose-point kernel values, the differences between dose values for each fetal percentile could be analytically described. As shown in figure 6, the DPK ratios (with respect to 50th percentile) confirmed the ratios between corresponding Monte Carlo-based estimations. Furthermore, an obvious increasing or decreasing trend was not observed for ^{99m}Tc-Technegas because the role of self-dose is predominantly canceling the effect of cross dose variations.

Another essential point is the determination of absorbed dose (Gy) using dose coefficients (Gy/MBq) and administered activity (MBq). In this respect, the typical administered activities of 60, 80, and 40 MBq were assumed for ^{99m}Tc-MAA, aerosol ^{99m}Tc-DTPA and ^{99m}Tc-Technegas, respectively and corresponding absorbed doses were used to verify two important issues. Firstly, it was pursuing that if any of dose points exceeds the threshold of 1 mGy for which a risk of secondary childhood cancer was reported. Secondly, to explore whether consideration of fetal percentiles in the calculation of absorbed doses is dosimetrically relevant. To answer these questions, dose points were plotted in figure 5 together with 95% confidence and prediction intervals.

This figure shows that for the typical administered activities of 60, 80, and 40 MBq for ^{99m}Tc-MAA, aerosol ^{99m}Tc-DTPA and ^{99m}Tc-Technegas, respectively, dose values are well below the dose threshold (i.e., 10 mGy) above which there is increased risk of childhood cancer for the unborn child. At diagnostic level, the primary concern for the fetus is an increased risk (0.06% per mGy) of leukemia or childhood cancer following in-utero exposure, which is reported for doses above 10 mGy [30]. Therefore, there should be no concern about the fetal body habitus and reference values for the 50th percentile could be safely used in the case of administration of the three considered radiopharmaceuticals in this study.

Conclusion

Fetal dose coefficients are dependent on many factors such as anatomical and physiological parameters of both pregnant woman and the fetus. The effect of these uncertainty components was not yet fully investigated. This study aimed to investigate the effect of different fetal body habitus subgroups on the variation of fetal dose. Furthermore, we aimed to investigate whether the dose variation is clinically relevant or not. The results showed that the dose variations were well below the safety threshold for the fetus (i.e., 10 mGy), at which the risk of fetal cancer is not statistically negligible. Therefore, to check the safety of the test in terms of radiation dose to the fetus, it is sufficient to take into account the reference dose values in clinical practice and there should be no concern about the fetal body habitus. The reference values for the fetus at 50th percentile could be safely used in the case of administration of the three considered radiopharmaceuticals in this study.

References

1. Cantwell R, Clutton-Brock T, Cooper G, et al. Saving mothers′ lives: reviewing maternal deaths to make motherhood safer: 2006-2008. The eighth report of the confidential enquiries into maternal deaths in the United Kingdom. BJOG. 2011; 118 (suppl 1): 1–203.
2. Mallick S, Petkova D. Investigating suspected pulmonary embolism during pregnancy. Respir Med. 2006; 100: 1682–87.
3. James AH, Bushnell CD, Jamison MG, Myers ER. Incidence and risk factors for stroke in pregnancy and the puerperium. Obstet Gynecol. 2005; 106:509–16.
4. James AH, Jamison MG, Biswas MS, Brancazio LR, Swamy GK, Myers ER. Acute myocardial infarction in pregnancy: a United States population-based study. Circulation. 2006; 113:1564–71.
5. James AH. Venous thromboembolism in pregnancy. Arterioscler Thromb Vasc Biol. 2009; 29:326–31.
6. Committee on Practice Bulletins: Gynecology, American College of Obstetricians and Gynecologists. ACOG Practice Bulletin No 84 Prevention of deep vein thrombosis and pulmonary embolism. Obstet Gynecol. 2007; 110(2 Pt 1):429–40.
7. Mclintock C, Brighton T, Chunilal S, Dekker G, Mcdonnell N, Mcrae S, et al. Recommendations for the diagnosis and treatment of deep venous thrombosis and pulmonary embolism in pregnancy and the postpartum period. Australian and New Zealand Journal of Obstetrics and Gynaecology. 2012 Feb;52(1):14-22.
8. Leung AN, Bull TM, Jaeschke R, Lockwood CJ, Boiselle PM, Hurwitz LM, et al. American Thoracic Society documents: an official American Thoracic Society/Society of Thoracic Radiology Clinical Practice Guideline–evaluation of suspected pulmonary embolism in pregnancy. Radiology. 2012; 262: 635–46.
9. Bajc M, Neilly JB, Miniati M, Schuemichen C, Meignan M, Jonson B. EANM guidelines for ventilation/perfusion scintigraphy: Part 2. Algorithms and clinical considerations for diagnosis of pulmonary emboli with V/P(SPECT) and MDCT. Eur J Nucl Med Mol Imaging. 2009; 36: 1528–38.
10. Konstantinides SV, Meyer G, Becattini C. 2019 ESC Guidelines for the diagnosis and management of acute pulmonary embolism developed in

collaboration with the European Respiratory Society (ERS): The Task Force for the Diagnosis and Management of Acute Pulmonary Embolism of the European Society of Cardiology (ESC). Eur Respir J 2019; 54: 2019.
11. Linnemann B, Bauersachs R, Rott H, Halimeh S, Zotz R, Gerhardt A,et al. Diagnosis of pregnancy associated venous thromboembolism—position paper of the Working Group in Women′s Health of the Society of Thrombosis and Haemostasis (GTH). Vasa 2016; 45: 87–101.
12. Royal College of Obstetricians and Gynaecologists. Thromboembolic disease in pregnancy and the puerperium: acute management. Green-top Guideline No. 37b. 2015. Available from: https://www.rcog.org.uk/ globalassets/documents/guidelines/gtg-37b.pdf (accessed Nov 26, 2019).
13. Chan WS, Rey E, Kent NE, Corbett T, David M, Douglas MJ, et al. Venous thromboembolism and antithrombotic therapy in pregnancy. J Obstet Gynaecol Can 2014; 36: 527–53.
14. Bajc M, Olsson B, Gottsäter A, Hindorf C, Jögi J. V/P SPECT as a diagnostic tool for pregnant women with suspected pulmonary embolism. European journal of nuclear medicine and molecular imaging. 2015 Jul;42(8):1325-30.
15. Perisinakis K, Seimenis I, Tzedakis A, Damilakis J. Perfusion scintigraphy versus 256 -slice CT angiography in pregnant patients suspected of pulmonary embolism: comparison of radiation risks. Journal of Nuclear Medicine. 2014 Aug 1;55(8):1273 -80.
16. Niemann T, Nicolas G, Roser HW, Müller-Brand J, Bongartz G. Imaging for suspected pulmonary embolism in pregnancy—what about the fetal dose? A comprehensive review of the literature. Insights into imaging. 2010 Nov;1(5):361-72.
17. Vakili S, Shahbazi-Gahrouei D, Pourasbaghi P, Raeisi E. Investigation of fetal absorbed dose in V/Q scan in three trimesters of pregnancy using Monte Carlo simulation. World Journal of Nuclear Medicine. 2021 Oct;20(4):342.
18. Rafat Motavalli L, Hoseinian Azghadi E, Miri Hakimabad H, Akhlaghi P. Pulmonary embolism in pregnant patients: assessing organ dose to pregnant phantom and its fetus during lung imaging. Medical physics. 2017 Nov;44(11):6038-46.
19. Motavalli LR, Hakimabad HM, Azghadi EH. Fetal and maternal dose assessment for diagnostic scans during pregnancy. Physics in Medicine & Biology. 2016 Apr 13;61(9):3596.
20. Rafat-Motavalli L, Miri-Hakimabad H, Hoseinian-Azghadi E. Dosimetric factors for diagnostic nuclear medicine procedures in a non-reference pregnant phantom. Journal of Radiological Protection. 2018 Jun 7;38(3):908.
21. ICRP Publication 89. Basic anatomical and physiological data for use in radiological protection: reference values, Ann. ICRP 32 (3 -4). 2002.
22. Rafat-Motavalli L, Miri-Hakimabad H, Hoseinian-Azghadi E. Hybrid pregnant reference phantom series based on adult female ICRP reference phantom. Radiation Physics and Chemistry. 2018 Mar 1;144:386-95.
23. Hoseinian-Azghadi E, Rafat-Motavalli L, Miri-Hakimabad H. Development of a 9-months pregnant hybrid phantom and its internal dosimetry for thyroid agents. Journal of radiation research. 2014 Jul 1;55(4):730-47.
24. Hendricks JS, McKinney GW, Fensin ML, James MR, Johns RC, Durkee JW, et al. MCNPX 2.6. 0 Extensions. Los Alamos National Laboratory. 2008 Apr 11:73.
25. Taranenko V, Zankl M, Schlattl H. Voxel phantom setup in MCNPX. InProc. Monte Carlo 2005 topical meeting. The Monte Carlo method: versatility unbounded in a dynamic computing world (17–21 April 2005, Chattanooga, TN). 2005 Apr.
26. Hoseinian-Azghadi E, Rafat-Motavalli L, Miri-Hakimabad H. Internal dosimetry estimates using voxelized reference phantoms for thyroid agents. Journal of Radiation Research. 2014 May 1;55(3):407-22.
27. Russell JR, Stabin MG, Sparks RB. Placental transfer of radiopharmaceuticals and dosimetry in pregnancy. Health physics. 1997 Nov 1;73(5):747-55.
28. Martin JE. Physics for radiation protection: a handbook. John Wiley & Sons; 2006.
29. XCOM database available at https://atom.kaeri.re.kr/cgi-bin/w3xcom
30. Russell JR, Stabin MG, Sparks RB, Watson E. Radiation absorbed dose to the embryo/fetus from radiopharmaceuticals. Health physics. 1997 Nov 1;73(5):756-69.
31. Parker JA, Coleman RE, Grady E, Royal HD, Siegel BA, Stabin MG, et al. SNM practice guideline for lung scintigraphy 4.0. Journal of nuclear medicine technology. 2012 Mar 1;40(1):57-65.
32. ICRP, 2000. Pregnancy and Medical Radiation. ICRP Publication 84. Ann. ICRP 30 (1).
33. Doll R, Wakeford R. Risk of childhood cancer from fetal irradiation. The British journal of radiology. 1997 Feb;70(830):130-9.